University of Liege - Faculty of Applied Sciences
Structural Engineering Research Unit

Validation of SAFIR® through DIN EN 1992-1-2 NA

Comparison of the results for the examples presented in Annex CC

March 2017

J. Ferreira
J.-M. Franssen
T. Gernay

University of Liege - ArGEnCo - *Structural Engineering*
Institut de Mécanique et Génie Civil
Allée de la Découverte, 9 - 4000 Liège - Belgium
Sart Tilman - Bâtiment B52 - Parking P52
www.argenco.ulg.ac.be

Tél.: +32 (0)4 366.92.65
+32 (0)4 366.92.53
Fax: +32 (0)4 366.95.34
E-mail : jm.franssen@ulg.ac.be
Thomas.Gernay@ulg.ac.be

Table of contents

1. Introduction

1.1. Form of validation

Annex CC of DIN EN 1992-1-2 NA presents a series of cases that allow benchmarking software tools aimed at the design of structures in a fire situation.

With the goal of providing a validation document for the finite element code SAFIR, a comparison of the reference results for the cases presented in the Annex CC with the results obtained by SAFIR has been carried out and is presented in this document.

The validation typically consists in a comparison between the value of a result (temperature, displacement or others) obtained by SAFIR and the value given as a reference and supposed to be the « *true* » result. The value obtained must fall in the interval stipulated by the document.

1.2. Structure of the document

This document contains comparisons of SAFIR with the examples provided by the DIN. For each example, keywords are initially provided in order to easily detect what is being analysed in the example. The objective of the example is then summarized and a description of the necessary information concerning geometry, boundary conditions, loads, parameters, material laws, etc, is given. Finally, a description of the model used and possible assumptions is presented and the main conclusions about the comparisons of SAFIR to the reference solutions are exposed.

All the SAFIR files used are made available with this document, and references to the folders where they are located are given in the sub-chapters related to each model. The pictures that allow visualizing the results of SAFIR were made with the post-processor DIAMOND 2016, which can be downloaded for free on the SAFIR website.

1.3. Sources of differences in results

Some differences between the results of SAFIR and the reference values may be observed either due to different formulations being used or to the fact that some of the reference values actually come or are adjusted from experimental tests with their inherent variability. Other sources of differences are yet not due to the software itself but to the way the results are obtained and presented. This is discussed in the next two sections.

1.3.1 Significant digits

In many cases, the true value is a real number and its expression should involve an infinite number of significant digits, like for instance 0,034586235798412658951235 48… However, the determined value is always given with a certain resolution, i.e. a limited number of significant digits, and it is not always mentioned whether this has been obtained by rounding or by truncating the true value. In the example above, with only 2 significant digits, the rounded value is 0,035 whereas the truncated value is 0,034[1]. Such an uncertainty of 0,001 represents 2,857% of the

[1] This reference value of 0,034 is present in

Example 5 of DIN EN 1992-1-2.

rounded value and 2,941% of the truncated value whereas the maximum allowed deviation may be as low as 1%.

Moreover, the results produced by SAFIR have by default a limited number of significant digits (typically 8 or 16 digits). As it may not be relevant to print all results with such a high resolution, results are usually rounded before they are written in the two different files that are produced by SAFIR: *filename.out* and *filename.xml*. In these two files, the resolution may not be the same. For example, the displacements written in the *out* file, meant to be read by the human eye, are in 1/100 of a mm, which is supposed to be sufficiently small for a civil engineering structure. In the *xml* file, however, meant to be used by the graphic postprocessor Diamond, they are written with 3 significant digits.

In the exercises reported in this document, the value considered for SAFIR are always the most precise of both, based on the fact that any user has access to both files. For example, if the example above is a displacement in mm, SAFIR would write 0,00003 in the *out* file and 3,46E-03 in the *xml* file and the later would be used to calculate the deviation from the reference value. In this case, the double effect of rounding or truncating the reference value and of rounding the result of SAFIR would give a deviation of 1,14% with the rounded reference value and 1,76% with the truncated reference value, even if SAFIR calculates the true value to the 8th or 16th significant digit.

In some cases, it is possible to modify the size of the structure to be analysed in the reference case to obtain, at least, more significant digits in the *out* file produced by SAFIR. For example, the thermal expansion of a bar would be 10 times higher if the size of the bar is multiplied by 10. Interested users may want to do that, but this has not been done for this document.

1.3.1 Refinement of the model

The results calculated by a finite element software highly depend on the discretisation of the model in space, with finer grids yielding more correct results. If the analysis is transient, the results also depend on the discretisation in time, with smaller time steps yielding more correct results. The question of the discretisation to be used by the software, to produce the results that will be compared with the reference value, is typically not discussed in the documents that give the reference value.

In this exercise, the results are first presented with a model that is sufficiently refined (in space and in time) to ensure a converged solution, which means that the solution would not be different[2] with a finer model. Yet, it is highly valuable for the user to have an idea of the convergence of the solution when the model is "degraded". This allows answering the following question: what level of refinement is required for the software to yield acceptable results? This is why for some of the examples, in addition to the results produced with the converged model, we will present also results obtained with different levels of refinement. It must then come as no surprise if, when the model is too crude, the results don't fall within the acceptable limits anymore.

[2] Within the limits of the available resolution

1.4. Results versus visualisation

Results produced by SAFIR come in the form of numbers. In order to validate the software, these numbers are considered and compared to the reference values and the results of the comparisons are usually given in tables. Yet, in order to give a more intuitive feeling of the results, these results can also be processed in order to create drawings. The graphical tool DIAMONDS has been specifically developed at Liege University to create drawings based on SAFIR results and has been used in this report[3].

It has yet to be understood that some simplifications may be used to produce the drawings and these are discussed in this section.

1.4.1 Temperature field on triangular facets.

The temperature distribution on a triangular facet of a 3D SOLID element or on a triangular 2D SOLID element varies linearly. The graphic representation of the temperature distribution on such facets being linear is the exact representation of the temperature distribution considered in SAFIR, see Figure 12 for example.

The same holds for the representation of the warping function calculated for a torsion analysis.

1.4.2 Temperature field on quadrangular facets.

The temperature distribution on a quadrangular facet of a 3D SOLID element or on a quadrangular 2D SOLID element varies in a nonlinear manner. Being based on the temperature of the 4 nodes located at the corners of the facet, the temperature distribution is driven by an equation of the type given hereafter.

$$T(x,y) = k_1 + k_2\, x + k_3\, y + k_4\, xy$$

In order to accelerate the drawings, this nonlinear distribution is simplified in DIAMOND. The temperature at the centre of gravity of the facet T_c is calculated exactly as the average of the 4 corner temperatures. Then DIAMOND divides the quadrangle into 4 triangles, each one based on the centre of the quadrangle and 2 adjacent corner nodes, see Figure 1. A linear temperature distribution is then assumed and drawn in each of the 4 triangles, and this distribution is different from the real distribution considered in SAFIR. This effect of artificial linearization is clearly visible, for example, on Figure 30 a) and Figure 31 a).

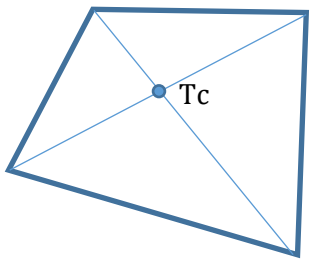

Figure 1 – Division of a quadrangle by DIAMOND

The same holds for the representation of the warping function calculated for a torsion analysis.

The visual effect of the approximation vanishes with the refinement of the mesh.

[3] Any other graphical software could be used provided it can read the XML file produced by SAFIR.

1.4.3 Representation of deformed beam elements

Beam finite elements in the deformed configuration are curved, because the end nodes are subjected to a rotation with respect to the chord that joints them. Yet, in order to simplify and to accelerate the drawing process, DIAMOND will draw each beam finite element as a straight line between the end nodes. Here again, the drawn situation does not correspond exactly to the situation considered in SAFIR.

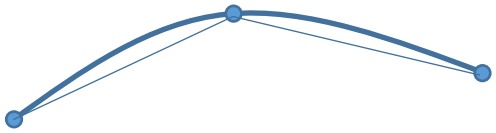

Figure 2 – Simplification of the drawn deformed configurations

In Figure 2, the thick curved line represents schematically a deformed configuration that could be considered by SAFIR whereas the two thin lines represent the configuration that would be drawn by DIAMOND for two beam finite elements.

Here also, the visual effect of the approximation vanishes with the refinement of the mesh.

2. Validation examples

2.1. Example 1

2.1.1 Keywords

Heat-transfer, conduction, convection, constant thermal properties

2.1.2 Objective

The goal of this example is to analyse the heat transfer by conduction and convection in a 2D square section with constant thermal properties.

2.1.3 Description of the problem

A square section with the characteristics defined in Figure 1 and Table 1 is here analysed. The temperature in the square section is uniform and equal to 1000°C at time t = 0 s when it is exposed to a gas with temperature = 0°C on one of the edges, the other edges being adiabatic. Heat transfer from the gas to the solid is by linear convection. In order to validate the results, the temperature θ_0 calculated at the centre of the opposite edge, at point X, is compared to the reference values presented in DIN EN1992-1-2 NA at different time instants.

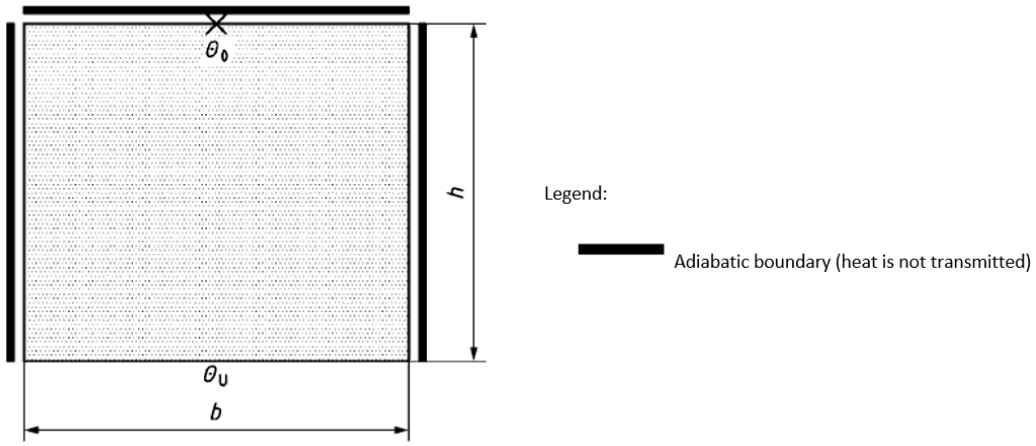

Figure 3 – Example 1: Cooling down process

Table 1 – Dimensions, material properties and boundary conditions for Example 1

Properties		Value
Thermal conductivity λ	W / (m·K)	1
Specific heat c_p	J / (kg·K)	1
Density ρ	Kg / m^3	1000
Dimensions h, b	M	1
Coefficient of convection α_c	W / (m^2·K)	1
Emissivity $\varepsilon_{res} = \varepsilon_m . \varepsilon_f$	-	0
Ambient temperature Θ_u	°C	0
Temperature in the cross-section Θ_{cs}	°C	1000

2.1.4 *Model and results (see folder DIN1_4)*

As the heat flow is uniaxial, from the exposed edge to the opposite edge, a model with only two rectangular elements on the width of the section is sufficient (in fact, a model with one single element on the width would yield the same answer, but it would not be possible to calculate the temperature at the centre node of the opposite edge). A structured mesh formed by 100 quadrilateral elements was used with 50 elements on the height, as depicted in Figure 4. Each of these elements contains 4 gauss points of integration (2x2) in its plane.

Figure 4 – Thermal model of the cross-section for Example 1 (2 x 50 SOLID elements)

In SAFIR, a "FRONTIER" constraint with the function "F0" was applied on the exposed edge, i.e. the lower edge in Figure 4 .

The "PRECISION" command was set to 1.0E-3. The material "INSULATION", having constant material properties, was used and given the properties described in Table 1.

The time step chosen was 1 second (final time / 1800.).

In Figure 5 is shown the distribution of the temperatures in the cross-section determined by SAFIR for the time t = 1800 s.

Table 2 shows the temperatures obtained by SAFIR and those given as reference by the DIN.

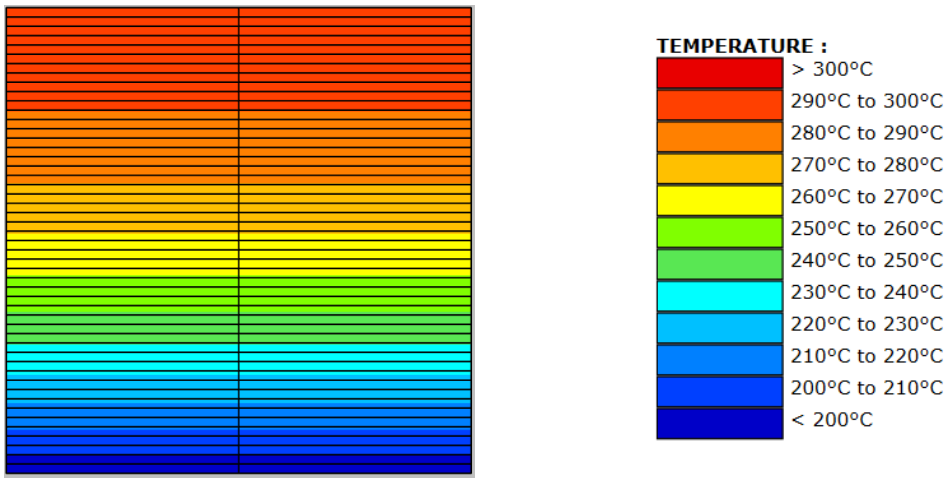

Figure 5 – Temperatures determined by SAFIR for Example 1, for t = 1800 s

Table 2 – Temperatures Θ_0 at point X for Example 1

Time	Reference temperature	Calculated temperature	Deviation	
t	Θ_0	Θ'_0	$(\Theta'_0 - \Theta_0)$	$(\Theta'_0 - \Theta_0) / \Theta_0 \cdot 100$
s	°C	°C	K	%
0	1000	1000	0.00	0.00
60	999.3	999.20	-0.10	-0.01
300	891.8	891.80	0.00	0.00
600	717.7	717.78	0.08	0.01
900	574.9	574.99	0.09	0.02
1200	460.4	460.52	0.12	0.03
1500	368.7	368.84	0.14	0.04
1800	295.3	295.42	0.12	0.04
Limits			±5.00	±1.00

It can be seen that the deviations fall well within the intervals of values defined in the DIN.

2.1.5 Analysis of the influence of different parameters

In this sub-chapter, an analysis of the sensibility of the results to different parameters is done. This will provide some indications on the minimal value of the time step or minimal number of nodes necessary in order to accurately simulate the cooling down process on the cross-section, as well as to confirm that the solution converges to a value as the mesh is refined.

2.1.5.1. Influence of the time step (see folder DIN1_5_1)

The mesh shown in Figure 5 was used here, and values of the time step equal to 1s, 5s, 10s, 20s, 30s, and 60s were tested. In Figure 4 are displayed the temperature distributions for four of these time steps, for the final time of 30min.

Figure 7 shows the evolution of the differences between the results from SAFIR and the ones of Annex CC as a function of time, depending on the value of the time step considered in the analysis.

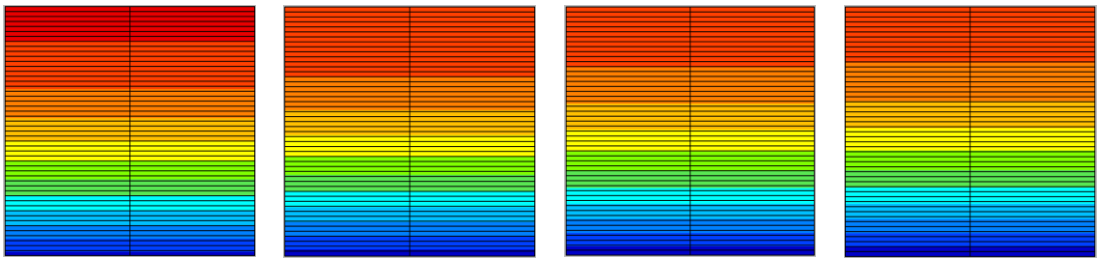

a) 60s b) 30s c) 10s d) 1s

Figure 6 – Temperatures determined by SAFIR for some of the time steps tested, for t = 1800s (colour scale is the same as in Figure 5)

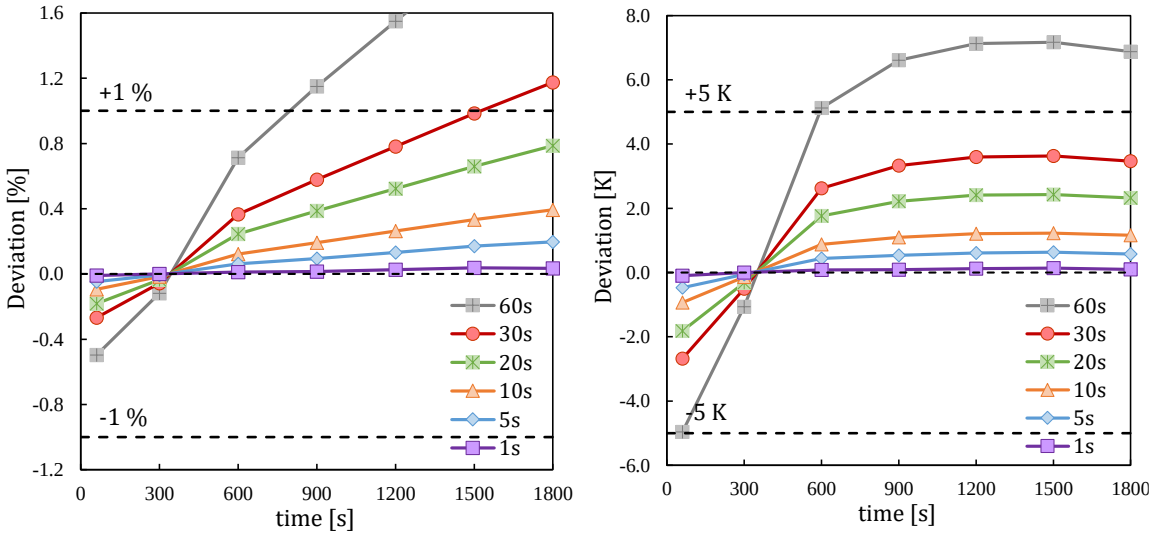

a) Percentage b) Degrees

Figure 7 – Differences between the results by SAFIR and the reference results for different time steps

Different observations can be made on the last Figure:

- Apart from the first 300s, the deviation is systematically positive;
- After 600s, the deviation in terms of % increases linearly with time;
- The deviation in terms of K seems to remain more or less constant after 600s;
- Both criteria given in DIN are met as long as the time step does not exceed 25 s (final time/72). If only the absolute difference in K is considered, a time step of 40 s (final time/45) is acceptable.

2.1.5.2. Influence of the number of nodes (see folder DIN1_5_2)

To assess the influence of the refinement of the mesh on the results, different meshes, with still two elements on the horizontal direction but a varying number of elements on the direction of the heat flow, are analysed here considering analyses with a time step = 1s.

In Figure 8 are shown some of the meshes that were used. The temperatures determined after 30 min are plotted in Figure 9 for the meshes in Figure 8. The results for the deviations from the DIN found for all the meshes tested are presented in Figure 10.

e) 2 x 2 (9 nodes) f) 2 x 8 (27 nodes) g) 2 x 20 (63 nodes) h) 2 x 100 (303 nodes)

Figure 8 – Some of the meshes used in the study regarding the influence of the number of nodes on the results

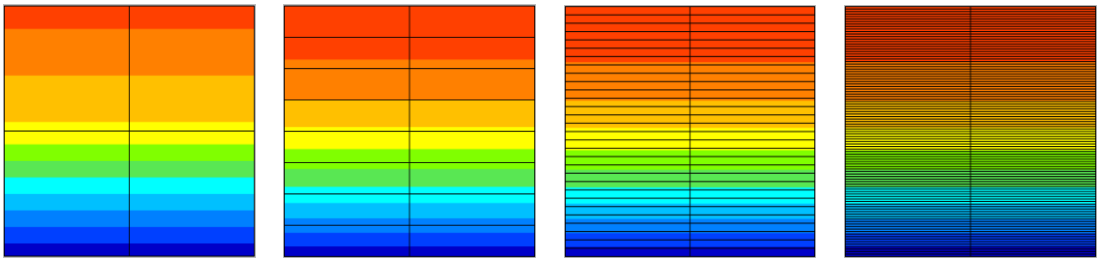

a) 2 x 2 (9 nodes) b) 2 x 8 (27 nodes) c) 2 x 20 (63 nodes) d) 2 x 100 (303 nodes)

Figure 9 – Temperatures determined by SAFIR for some of the meshes used to study the influence of the number of nodes, for t = 1800s (colour scale is the same as in Figure 5)

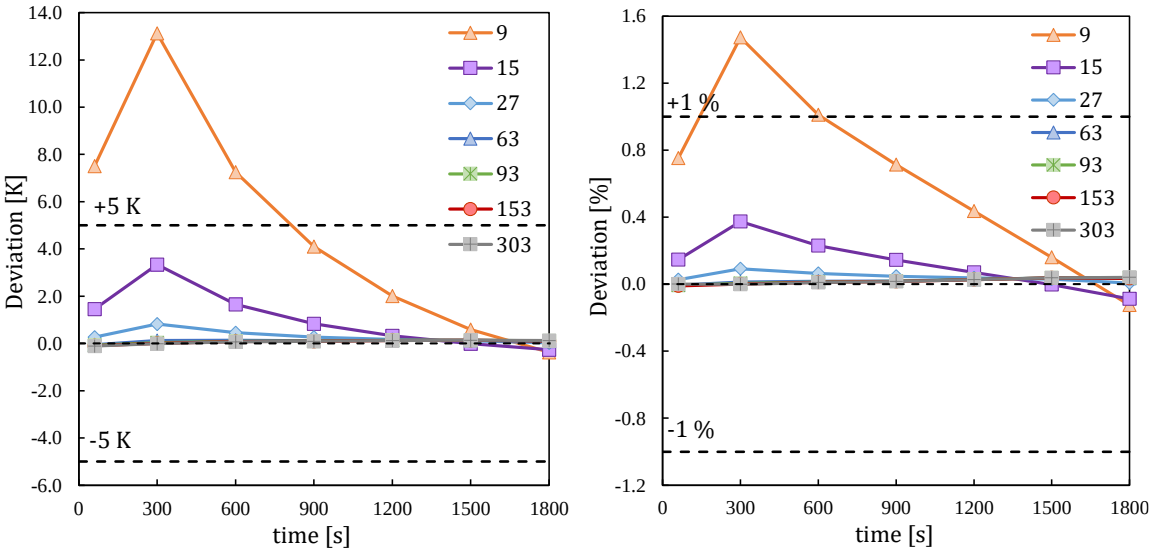

a) Degrees b) P

Figure 10 – Deviations of the results by SAFIR from the reference results for quadrilateral meshes with different densities (expressed in number of nodes)

Figure 10 shows that the models have converged when having more than 27 nodes (i.e. 7 nodes on the depth of the model), and that the results are within the limits defined in the DIN for meshes with as few as 4 nodes on the depth (or 15 nodes in total), if a grid configuration with two elements on the width is respected.

2.1.5.3. Influence of the element type (see folder DIN1_5_3)

A study was done in order to understand how the utilisation of triangles can affect the results. With that purpose, the crudest mesh from Figure 8 was taken as reference and triangle meshes with identical number and distribution of nodes were tested. Again, the time step here considered was for all cases equal to 1s.

The results for the temperatures at the top edge nodes of the cross-section are shown in Figure 11 and Figure 12 for t = 1800s, for the quadrilateral mesh and the meshes with triangles, respectively.

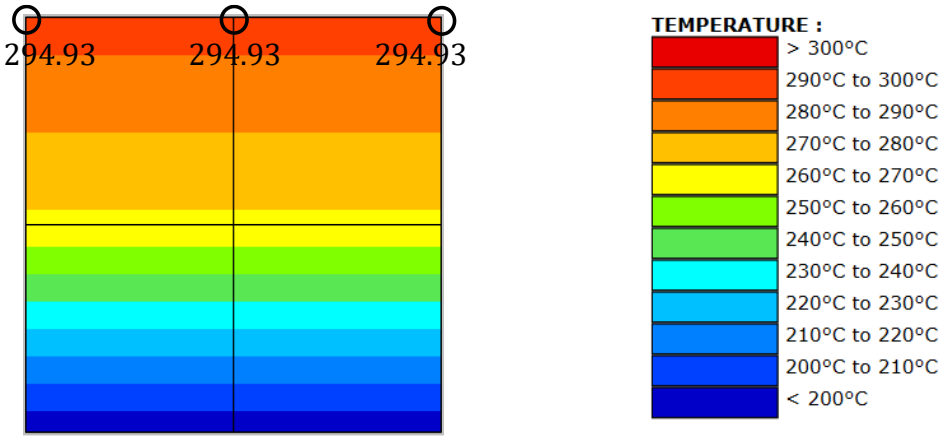

Figure 11 – Temperatures determined by SAFIR at the top 3 nodes for a quadrilateral mesh with 2x2 elements (9 nodes), for t = 1800s

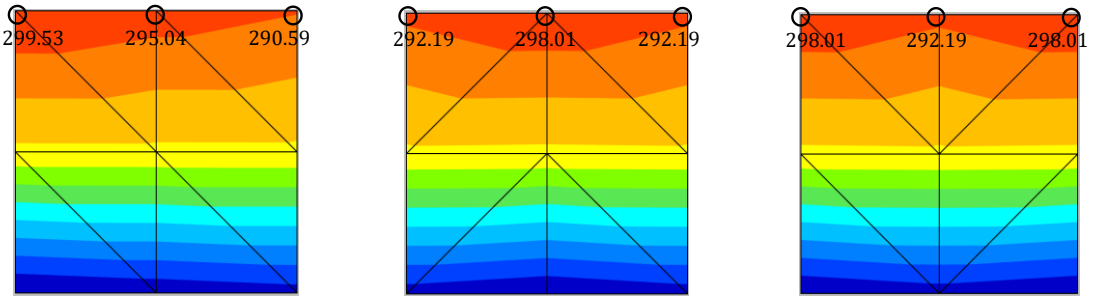

a) Mesh #1 b) Mesh #2 c) Mesh #3

Figure 12 – Temperatures determined by SAFIR at the top 3 nodes for three different triangle meshes with 9 nodes each for t = 1800s (colour scale is the same as in Figure 5)

It can be seen that for the three triangle meshes in Figure 12 the results depend on the arrangement of the triangles within the mesh, and that for the same mesh the nodes at the top edge show different values, unlike what happens with the quadrilateral mesh in Figure 11.

With a doubly symmetric mesh like the one in Figure 13, the same temperatures are obtained for the nodes with the same vertical position, as it is shown by the values plotted in that Figure for the top edge.

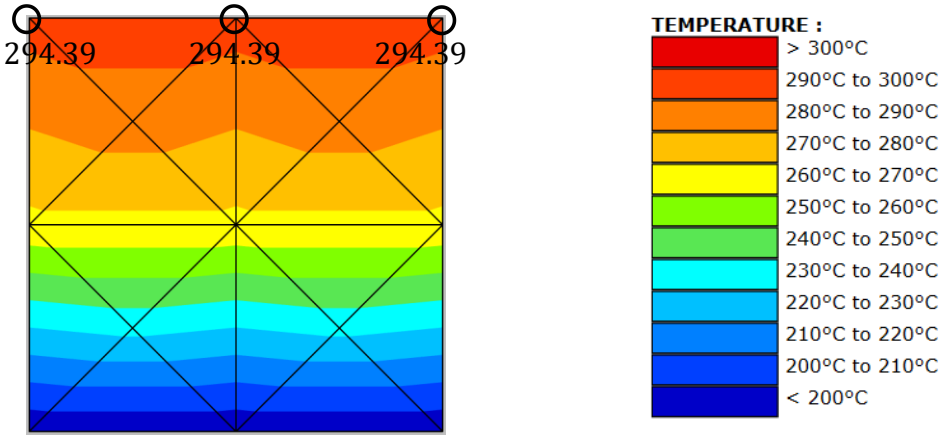

Figure 13 – Temperatures determined by SAFIR at the top 3 nodes for a doubly-symmetric triangle mesh with 13 nodes, for t = 1800s

Based on the latter, double symmetrical triangle meshes will be further compared to similarly refined models based on quadrilateral elements. For example, the triangle mesh in Figure 13 will be compared to the one presented in Figure 14.

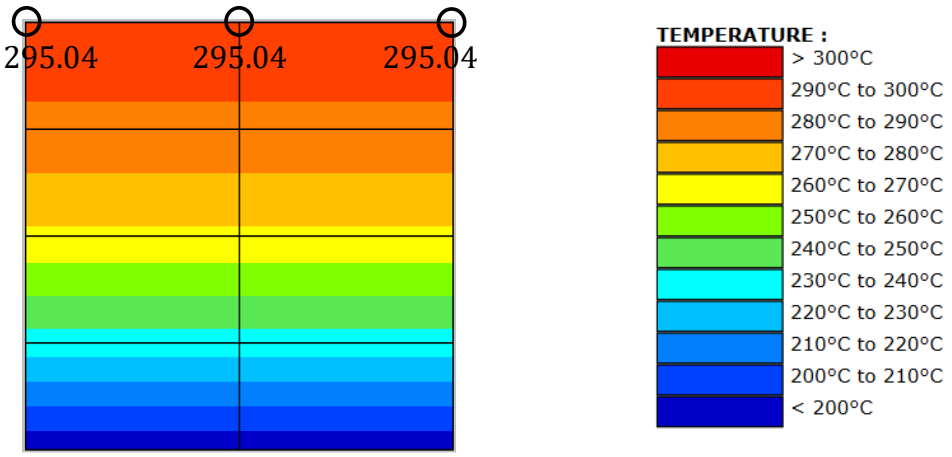

Figure 14 – Temperatures determined by SAFIR at the top 3 nodes for a quadrilateral mesh with 15 nodes, for t = 1800s

Figure 15 and Figure 16 show all the meshes tested. The distribution of the temperatures in the cross-sections are plotted in Figure 17 for t = 1800s, and the results for the temperature at the studied point are plotted in Figure 18.

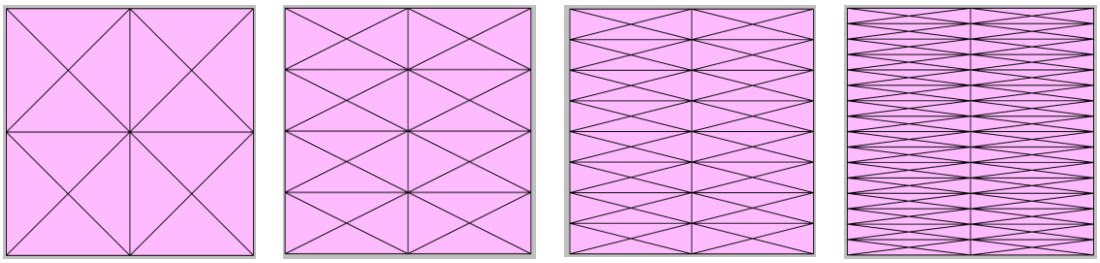

a) 13 nodes b) 23 nodes c) 43 nodes d) 83 nodes

Figure 15 – Triangle meshes used to study the influence of the type of element on the results

a) 15 nodes b) 27 nodes c) 51 nodes d) 99 nodes

Figure 16 – Quadrilateral meshes used to study the influence of the type of element on the results

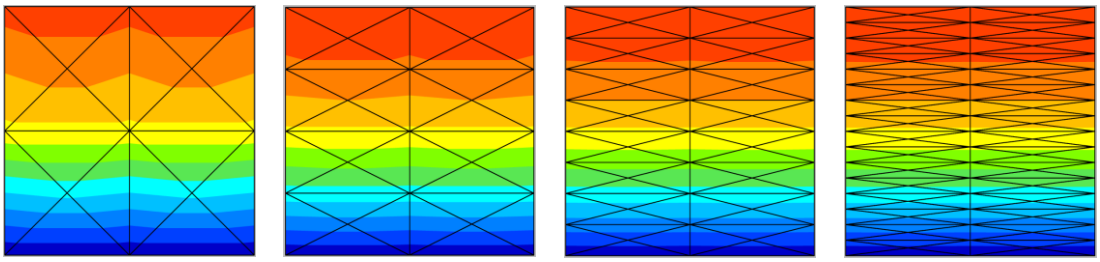

a) 13 nodes b) 23 nodes c) 43 nodes d) 83 nodes

Figure 17 – Temperatures determined by SAFIR for triangle meshes, for t = 1800s (colour scale is the same as in Figure 5)

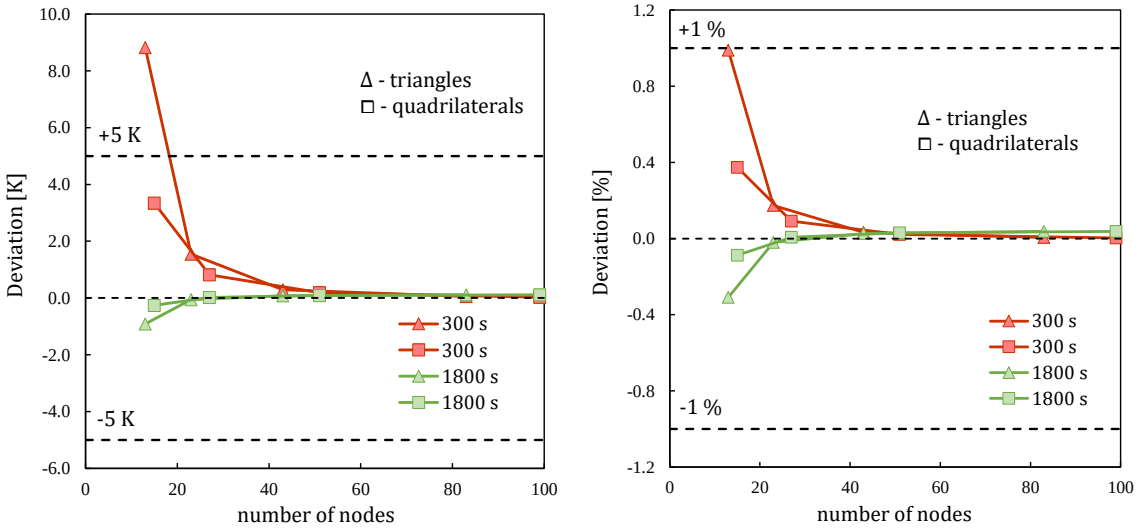

a) Degrees b) Percentage

Figure 18 – Deviations of the results by SAFIR from the reference results for meshes with triangles and quadrilateral elements (expressed in number of nodes)

By observing the plots in Figure 18 one can see that, for the two crudest meshes related to each element type, the ones with quadrilaterals return the more accurate results and seem to converge faster to the solution implemented in SAFIR. However, this should be at least partially justified by the difference on the number of nodes between the models with quadrilaterals and triangles. As for the other meshes tested, it seems that for meshes with more than 23 nodes a convergence on the results is attained, regardless of the element type.

As for finding the crudest mesh able to return valid results according to the DIN, based on the plots above a mesh formed with triangles with slightly more than 13 nodes seems to be sufficiently refined for that purpose.

2.1.5.4. Influence of distorted meshes (see folder DIN1_5_4)

In order to understand what is the impact of the distortion of elements in the mesh, the 4 meshes present in Figure 19 and their undistorted counterparts in Figure 20 were analysed, considering a time step = 1s. The distribution of the temperatures in the cross-section is plotted in Figure 21 for t = 1800s, and the deviations of the results from the DIN with both types of meshes can be found in Figure 22.

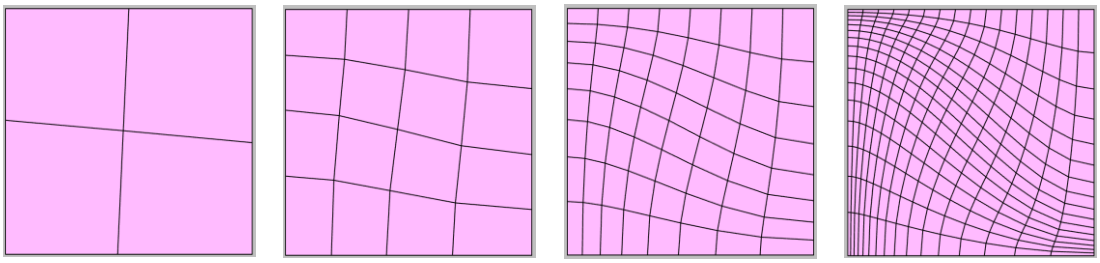

a) 9 nodes b) 25 nodes c) 81 nodes d) 289 nodes

Figure 19 – Distorted meshes used to study the influence of distortion of elements on the results

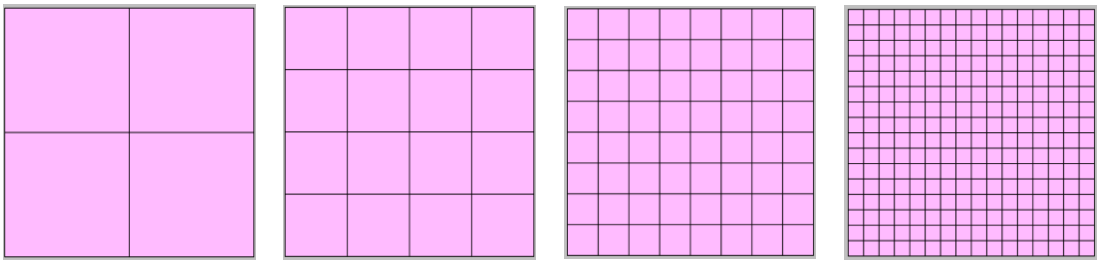

a) 9 nodes b) 25 nodes c) 81 nodes d) 289 nodes

Figure 20 – Undistorted meshes used to study the influence of distortion of elements on the results

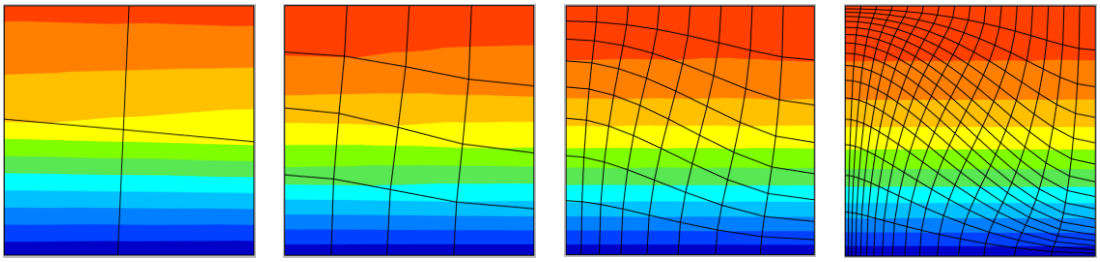

e) 9 nodes f) 25 nodes g) 81 nodes h) 289 nodes

Figure 21 – Temperatures determined by SAFIR for the distorted meshes, for t = 1800s (colour scale is the same as in Figure 5)

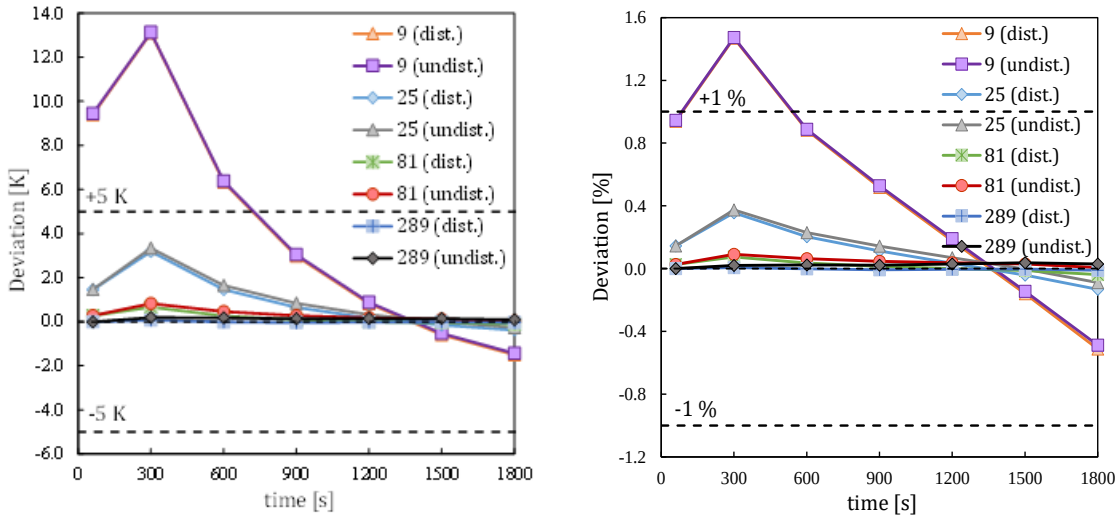

a) Degrees b) Percentage

Figure 22 –Deviations of the results by SAFIR from the reference results for the distorted and undistorted meshes (expressed in number of nodes)

By looking at Figure 22 it is seen that by using distorted meshes the results deviate only slightly from the ones obtained with equivalent undistorted meshes.

2.1.5.5. Influence of unstructured meshes (see folder DIN1_5_5)

As a last step of this parametric analysis, the influence of using unstructured meshes is investigated. The 6 unstructured meshes present in Figure 23 are analysed, again considering a time step = 1s. The distribution of the temperatures in the cross-section is plotted in Figure 24 for t = 1800s, and the deviations of the results from the DIN with the studied unstructured meshes can be found in Figure 25.

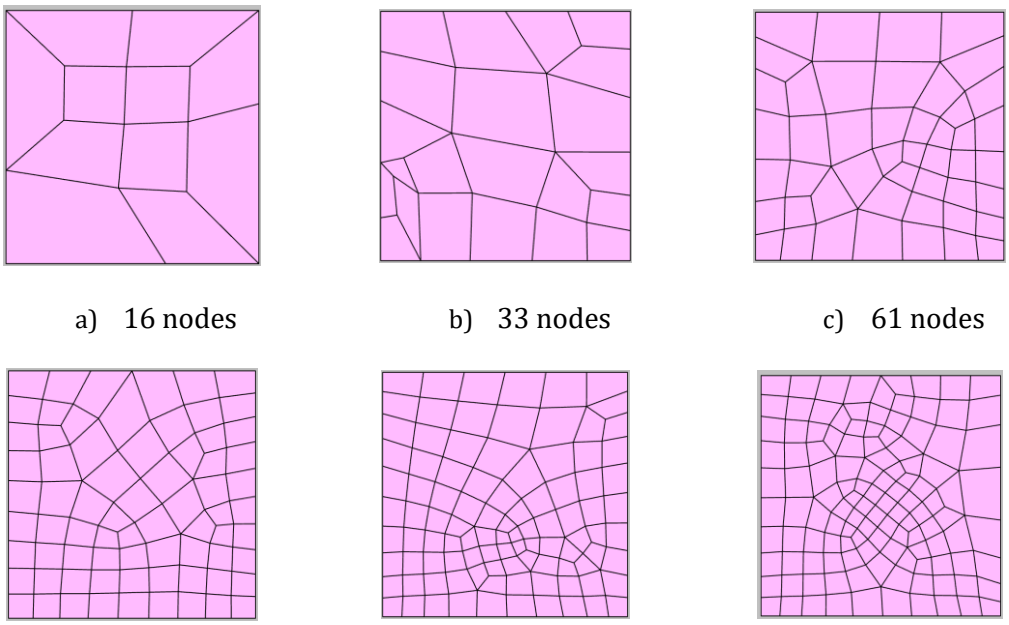

a) 16 nodes b) 33 nodes c) 61 nodes

d) 90 nodes e) 117 nodes f) 141 nodes

Figure 23 – Meshes used to study the influence of unstructured meshes on the results

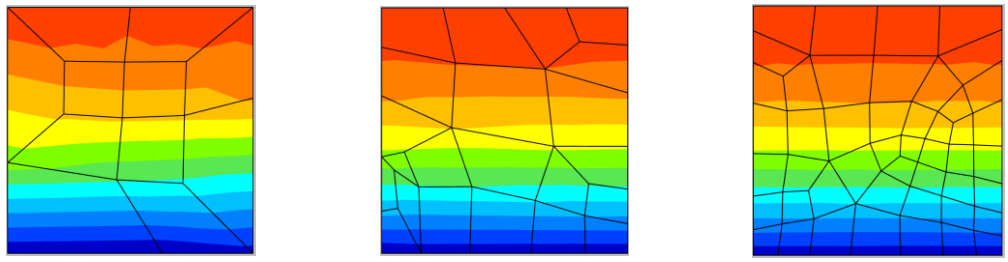

a) 16 nodes b) 33 nodes c) 61 nodes

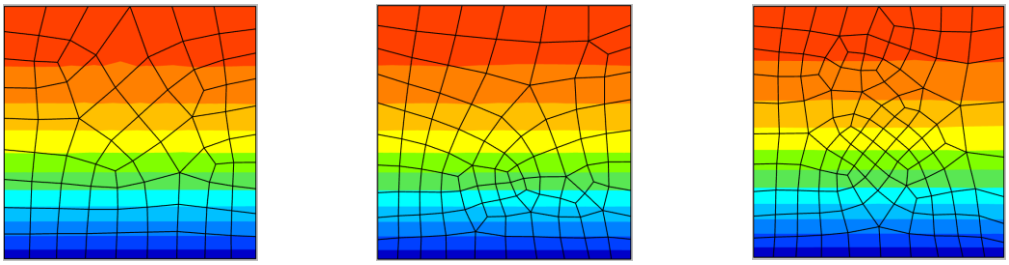

d) 90 nodes e) 117 nodes f) 141 nodes

Figure 24 – Temperatures determined by SAFIR for the unstructured meshes, for t = 1800s (colour scale is the same as in Figure 5)

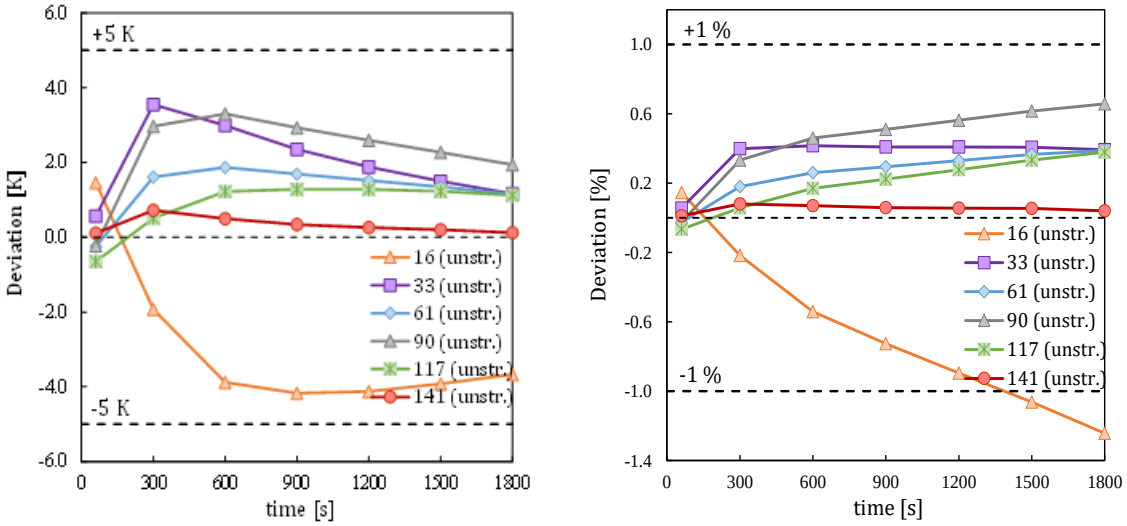

a) Degrees b) Percentage

Figure 25 –Deviations of the results by SAFIR from the reference results for the unstructured meshes (expressed in number of nodes)

One can observe from Figure 25 that:

- Overall, the results with unstructured meshes are well placed inside the stipulated values;
- Crude unstructured meshes like the one with 16 nodes therein present can lead to some deviations from the reference results (although relatively small);

- Unstructured meshes are less efficient and often require more nodes to attain the same level of results than structured ones, as it is proved by the fact that the unstructured mesh with 113 nodes in Figure 25 still presents some considerable deviations, whereas in Figure 22 a mesh with just 81 nodes was able to attain very close results to the ones found in the DIN;
- A very good agreement between the results from SAFIR and the DIN was achieved when using an unstructured mesh with 141 nodes.

2.1.6 Conclusions

The parametric analysis shows that the solution of SAFIR satisfies the requirement of the standard. The solution converges to the theoretical solution when the density of the mesh is increased and the value of the time step is reduced.

When refining the mesh, rectangular elements converge slightly faster than triangular element; regular structured meshes are most efficient, with slight differences being observed in distorted structured meshes; unstructured meshes are somehow less efficient while being still in the acceptable range of the standard.

2.2. Example 2

2.2.1 Keywords

Heat-transfer, conduction, convection, radiation, varying thermal properties

2.2.2 Objective

The goal of this example is to analyse the heat transfer by conduction when the thermal conductivity varies with the temperature, as well as the heat exchange with a gas at the boundary of the section by convection.

2.2.3 Description of the problem

A square section with the characteristics defined in Figure 26 and Table 3 is analysed. The temperature in the cross-section is uniform and equal to 0°C at time t = 0, when it is exposed to a gas with a temperature of 1000°C on all the edges. Heat transfer from the gas to the solid is by linear convection and radiation. In order to validate the results, the temperature θ_0 calculated at the centre of the cross-section is compared to the reference values presented in the DIN EN1992-1-2 NA at different times for a total duration of 3 hours.

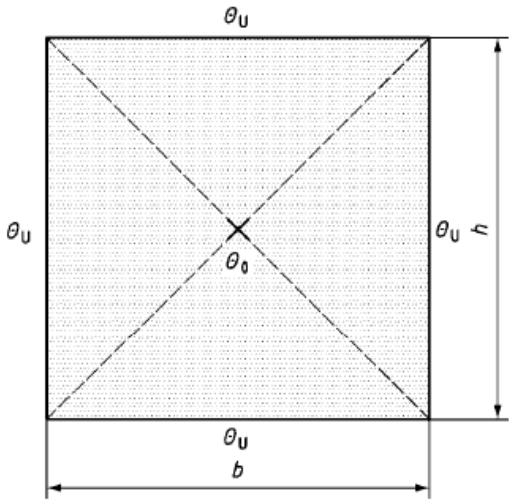

Figure 26 – Example 2: Heating process

Table 3 – Dimensions, material properties and boundary conditions for Example 2

Properties		Value	
Thermal conductivity λ (linear behaviour)	W / (m·K)	Θ	λ (Θ)
		0	1.5
		200	0.7
		1000	0.5
Specific heat c_p	J / (kg·K)	1000	
Density ρ	Kg / m³	2400	
Dimensions h, b	m	0.2	
Coefficient of convection α_c	W / (m²·K)	10	
Emissivity $\varepsilon_{res} = \varepsilon_m . \varepsilon_f$	-	0.8	
Ambient temperature Θ_u	°C	1000	
Initial temperature in the cross-section Θ_{cs}	°C	0	

The data of this exercise are similar to those of a 20x20 cm^2 concrete section.

2.2.4 *Model and results (see folder DIN2_4)*

A model with a structured mesh formed by 576 square elements (24 by 24) was created. Each of these elements contains 2 gauss points of integration in its plane, and the total number of nodes is 625.

The initial temperature in the structure was set to 0°C, and a FRONTIER constraint of 1000°C was applied to all faces of the cross-section by the function "F1000", as seen in Figure 27.

The PRECISION command was set to 1.0E-3. A USER material was applied according to the properties described in Table 4. The time step chosen was 10 seconds (final time / 1080).

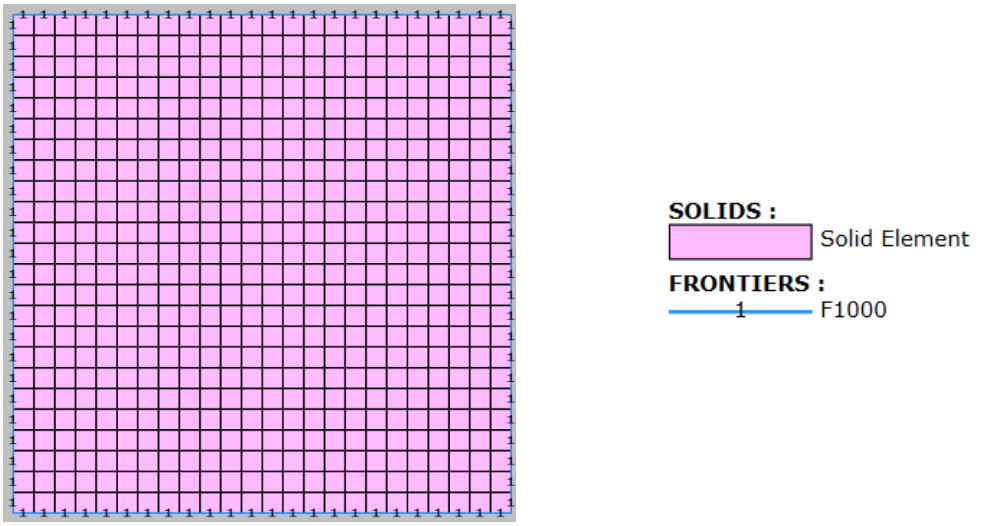

Figure 27 – Thermal model of the cross-section for Example 2 (24 x 24 SOLID elements)

Figure 28 shows the temperature distribution for the final target time of 180 min, whereas Table 4 gives the temperatures obtained by SAFIR and those given as reference by the DIN. All the differences are within the boundaries stipulated by the DIN.

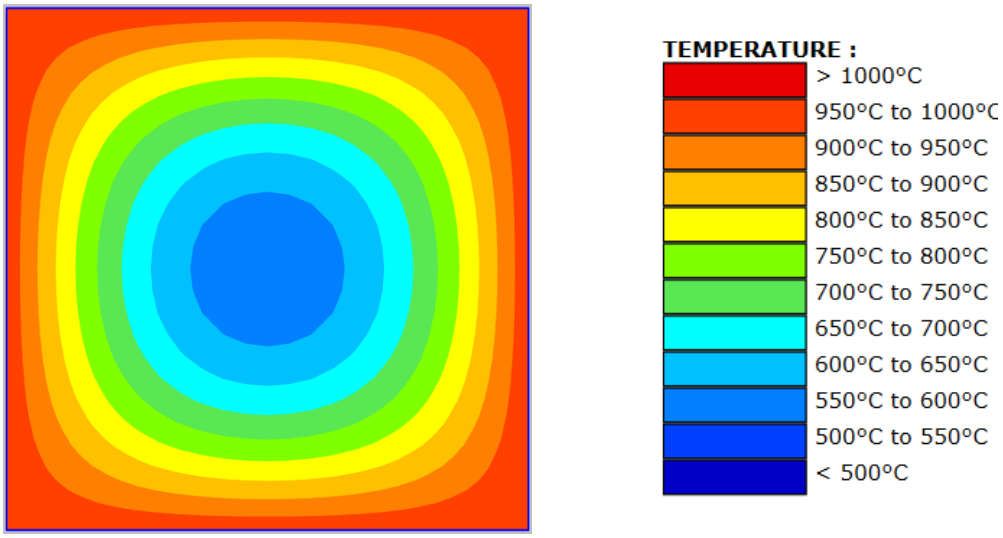

Figure 28 – Temperatures determined by SAFIR for Example 2, for t = 180min

Table 4 – Temperatures Θ_0 for Example 2

Time	Reference temperature	Calculated temperature	Deviation	
t	Θ_0	Θ'_0	$(\Theta'_0 - \Theta_0)$	$(\Theta'_0 - \Theta_0) / \Theta_0 \cdot 100$
min	°C	°C	K	%
30	36.9	32.18	-4.72	-12.79
60	137.4	132.40	-5.00	-3.64
Limit (t ≤ 60min)			±5.00	
90	244.6	241.67	-2.93	-1.20
120	361.1	362.75	1.65	0.46
150	466.2	469.83	3.63	0.78
180	554.8	559.93	5.13	0.92
Limit (t > 60min)				±3.00

2.2.5 *Analysis of the influence of different parameters*

In this sub-chapter, an analysis of the sensibility of the results to different input parameters is done. This will provide some indications on the minimal value of the time step or minimal number of nodes necessary in order to accurately simulate the heating process on the cross-section, as well as to confirm that the solution converges to a value as the mesh is refined.

2.2.5.1. *Influence of the time step (see folder DIN2_5_1)*

To study the influence of the time step on the results, the mesh shown in Figure 27 was used, and values of the time step equal to 1, 5, 10, 20, 30, 60, 120, 300, 600 and 1200 s were tested.

Figure 29 shows the evolution of the differences between the results from SAFIR and the ones of Annex CC as a function of time, depending on the value of the time step considered in the analysis. The areas of the chart with a white background represent the domain where the criteria, either in terms of percentage or in degrees, must be applied.

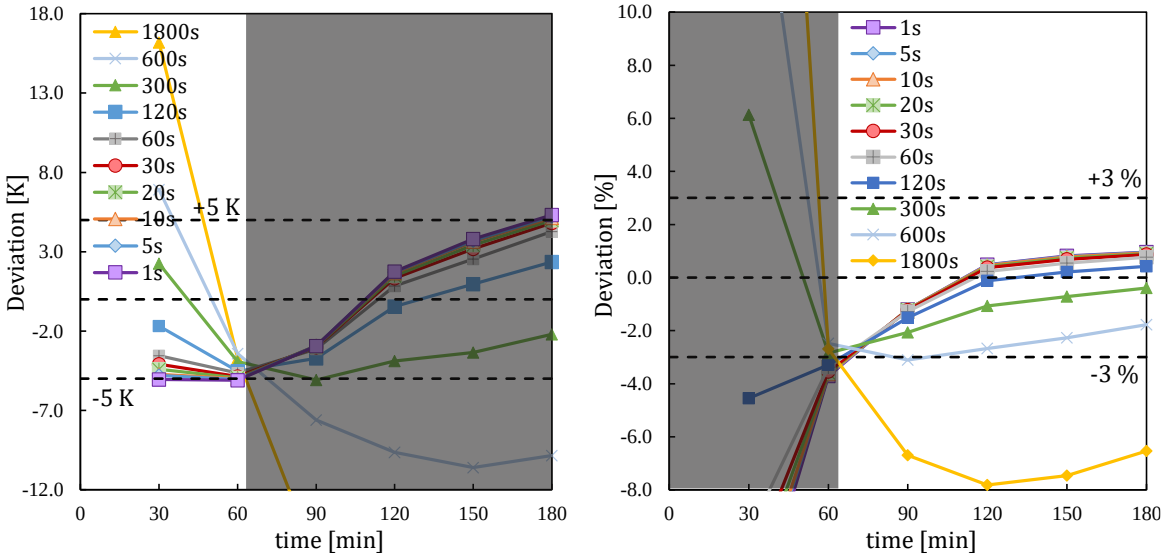

a) Degrees b) Percentage

Figure 29 – Differences between the results by SAFIR and the reference results for different time steps

Different observations can be made on the last Figure:

- For the values of the time steps between 1s and 300s, inclusive, all the results fall within the intervals, considering the zones of application of each criteria (percentage or Kelvin degrees);
- When considering the absolute difference in Kelvin, considerable differences between the different time steps are obtained for t = 30 min, where bigger time steps consistently return bigger temperatures. For this time instant, the time step that returns a temperature value identical to the reference seems to be somewhere between 120s and 300s. For t = 60 min these differences practically disappear.
- For the range of application of the limit in percentage, the results provided are valid for time steps of less than 600s, inclusive, with bigger time steps consistently returning lower temperatures, contrary to what happens for the first 60 min.

2.2.5.2. Influence of the number of nodes (see folder DIN2_5_2)

To assess the influence of the refinement of the mesh on the results, 6 different meshes are analysed considering analyses with a time step = 10s. All meshes were defined as a grid with equal number of elements in each direction, respectively 2x2, 4x4, 8x8, 16x16, 24x24 and 50x50.

Figure 30 shows part of the meshes that are used. The temperatures determined after 180 min are plotted in Figure 31 for those meshes. The results for the deviations from the DIN found for all the meshes tested are presented in Figure 32.

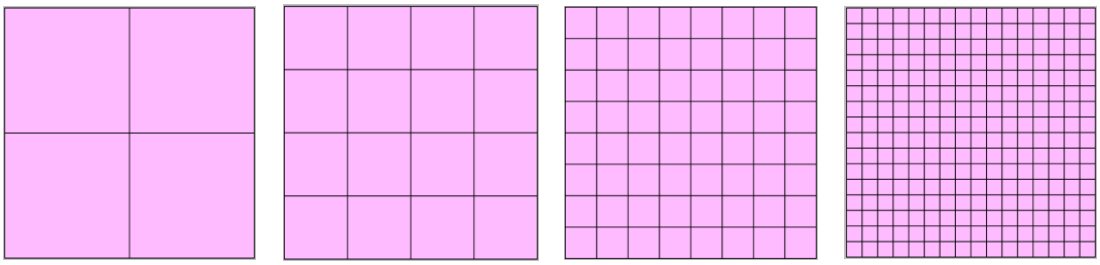

a) 2 x 2 (9 nodes) b) 4 x 4 (25 nodes) c) 8 x 8 (81 nodes) d) 16 x 16 (289 nodes)

Figure 30 – Meshes used to study the influence of unstructured meshes on the results

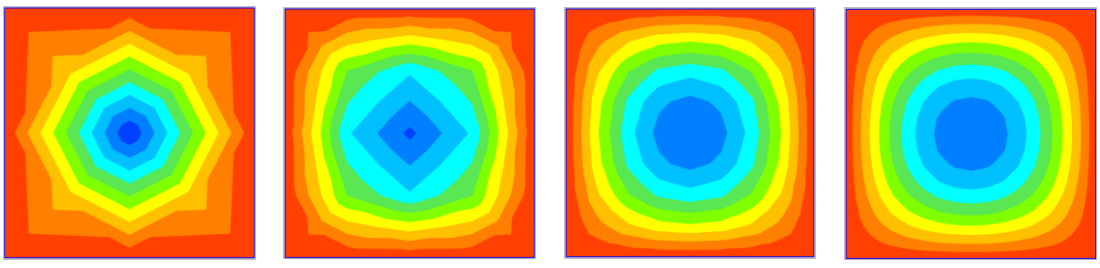

a) 2 x 2 (9 nodes) b) 4 x 4 (25 nodes) c) 8 x 8 (81 nodes) d) 16 x 16 (289 nodes)

Figure 31 – Temperatures determined by SAFIR for some of the meshes used to study the influence of the number of nodes, for t = 180min (colour scale is the same as in Figure 28)

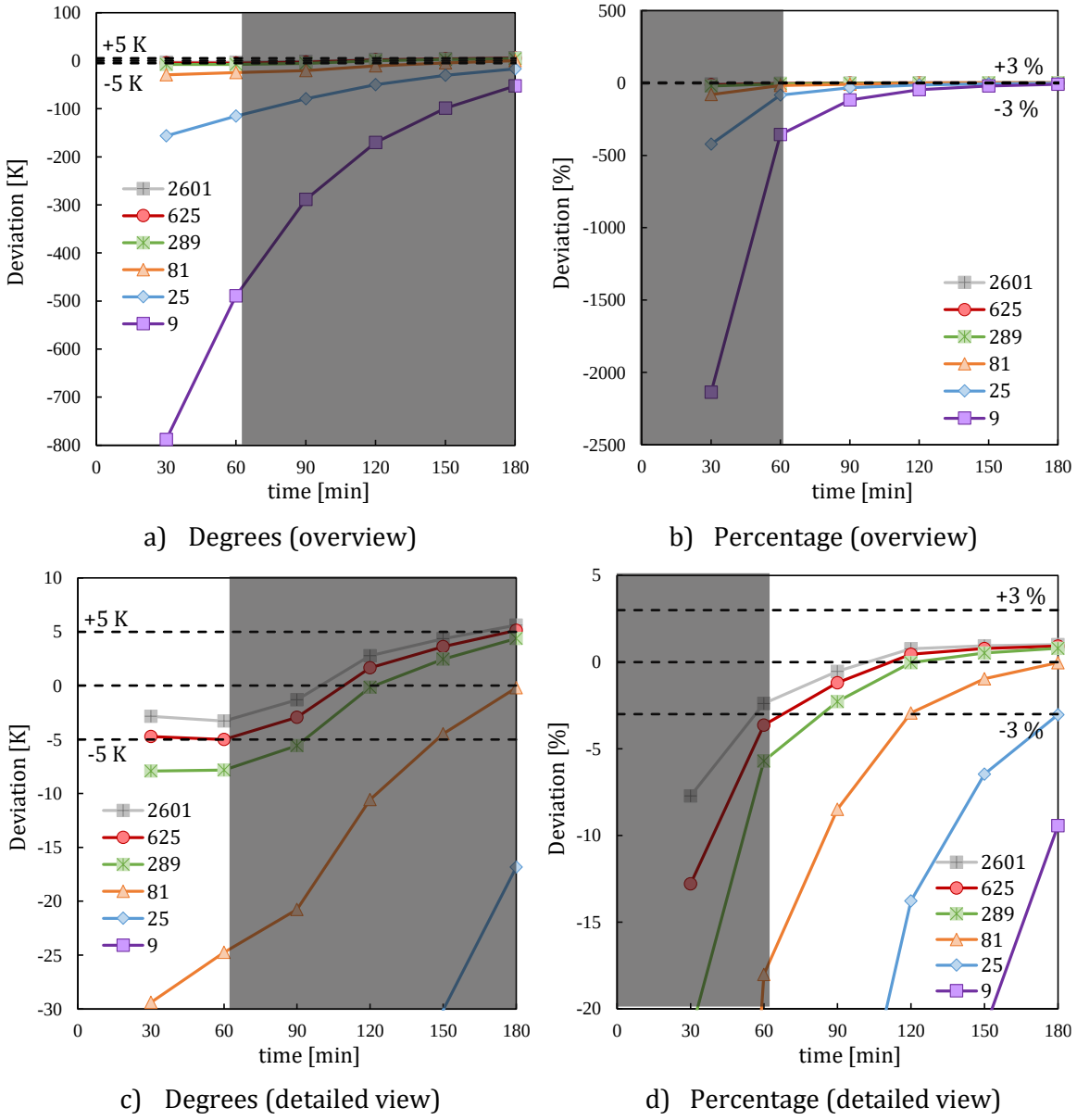

Figure 32 – Differences between the results by SAFIR and the reference results for quadrilateral meshes with different densities (expressed in number of nodes)

The following comments can be made on Figure 32:

- The crudest meshes analysed returned results that are hugely and negatively affected by the skin effect – the use of a reduced number of consecutive linear functions as an approximation to a parabolic solution;
- Considering the stipulated boundaries, meshes with at least 625 nodes are able to provide valid results for the whole range of time steps analysed (this corresponds to element thickness of 8.3 mm);
- The mesh with 289 nodes (12.5 mm thick elements) is able to provide good results for the range covered by the limitation in terms of percentage, but not for the one in terms of degrees.
- It seems therefore as if 10 mm is approximately the limit for the thickness of element layers near the surface in concrete type sections.

2.2.5.3. Influence of the element type (see folder DIN2_5_3)

The influence of the type of element is analysed here by means of 4 different triangle meshes compared with 4 quadrilateral meshes with a time step of 10 s.

Figure 33 and Figure 34 show the meshes tested. The distributions of the temperatures in the triangle meshes are plotted in Figure 35.

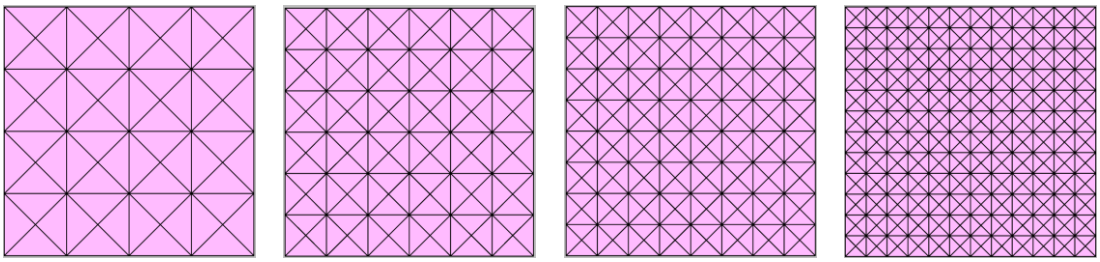

a) 41 nodes b) 85 nodes c) 145 nodes d) 313 nodes

Figure 33 – Triangle meshes used to study the influence of the type of element on the results

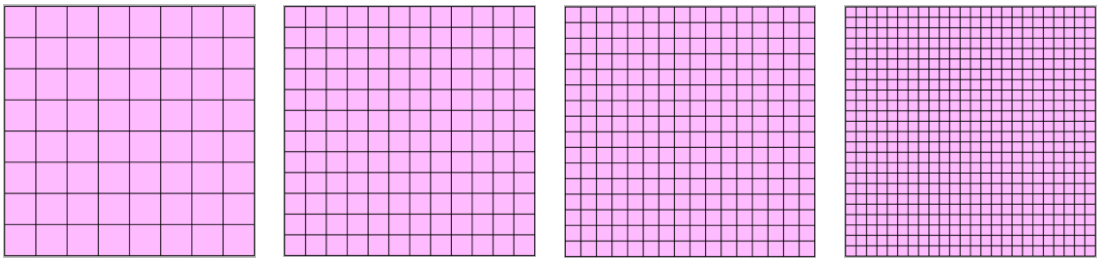

a) 81 nodes b) 169 nodes c) 289 nodes d) 625 nodes

Figure 34 – Quadrilateral meshes used to study the influence of the type of element on the results

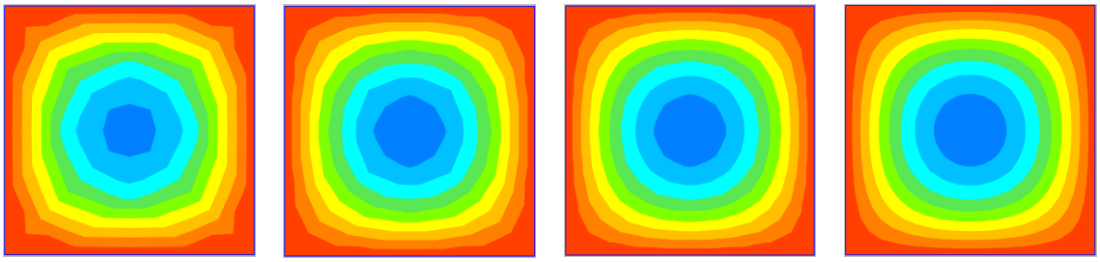

a) 41 nodes b) 85 nodes c) 145 nodes d) 313 nodes

Figure 35 – Temperatures determined by SAFIR for the triangle meshes, for t = 180 min (colour scale is the same as in Figure 28)

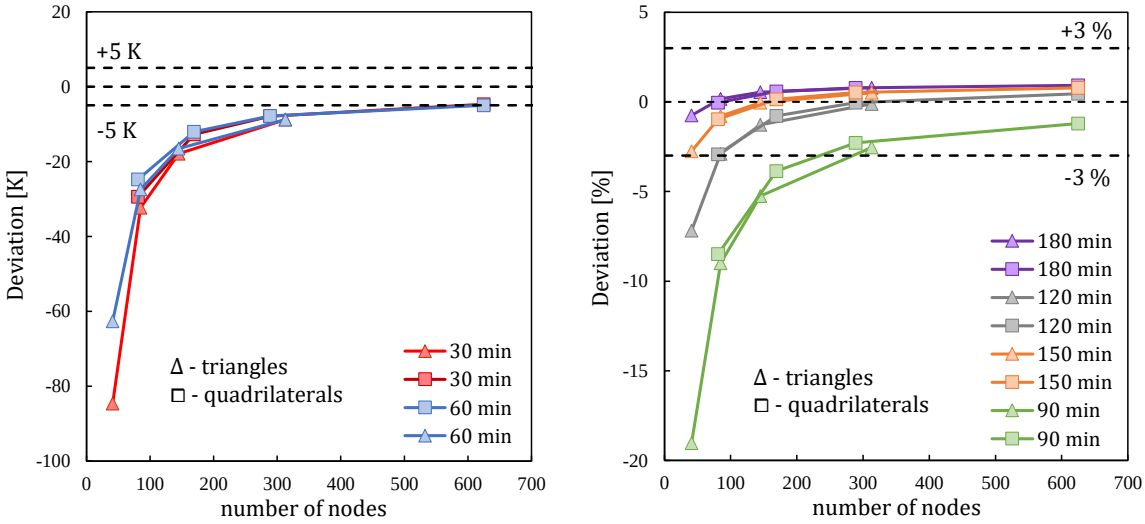

a) 30 and 60 min (in degrees)

b) 90, 120, 150 and 180 min (in percentage)

Figure 36 – Deviations of the results by SAFIR from the reference results for meshes with triangles and quadrilateral elements (expressed in number of nodes)

From Figure 40 it can be seen that the results between triangular elements and square elements are not significant (marginally better results are obtained with square elements).

2.2.5.4. Influence of unstructured meshes (see folder DIN2_5_4)

The influence of having unstructured meshes is investigated. The 4 meshes in Figure 37 were analysed, again considering a time step = 10s.

The distribution of the temperatures in the cross-section is plotted in Figure 38 for t = 180 min, and the deviations of the results from the DIN with the studied unstructured meshes can be found in Figure 39.

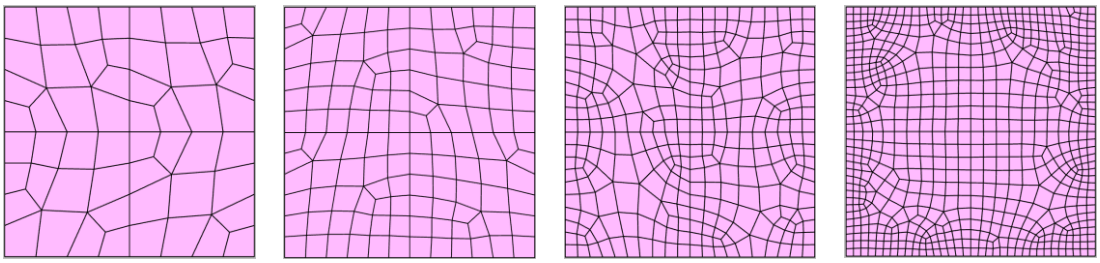

a) 72 nodes b) 153 nodes c) 355 nodes d) 743 nodes

Figure 37 – Meshes used to study the influence of unstructured meshes on the results

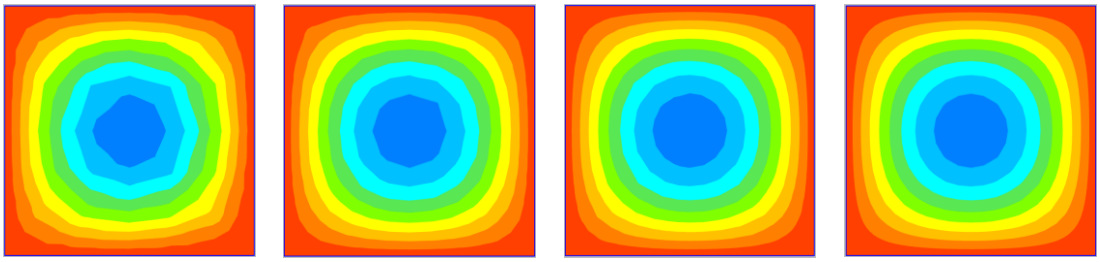

a) 72 nodes b) 153 nodes c) 355 nodes d) 743 nodes

Figure 38 – Temperatures determined by SAFIR for the unstructured meshes, for t = 180 min (colour scale is the same as in Figure 28)

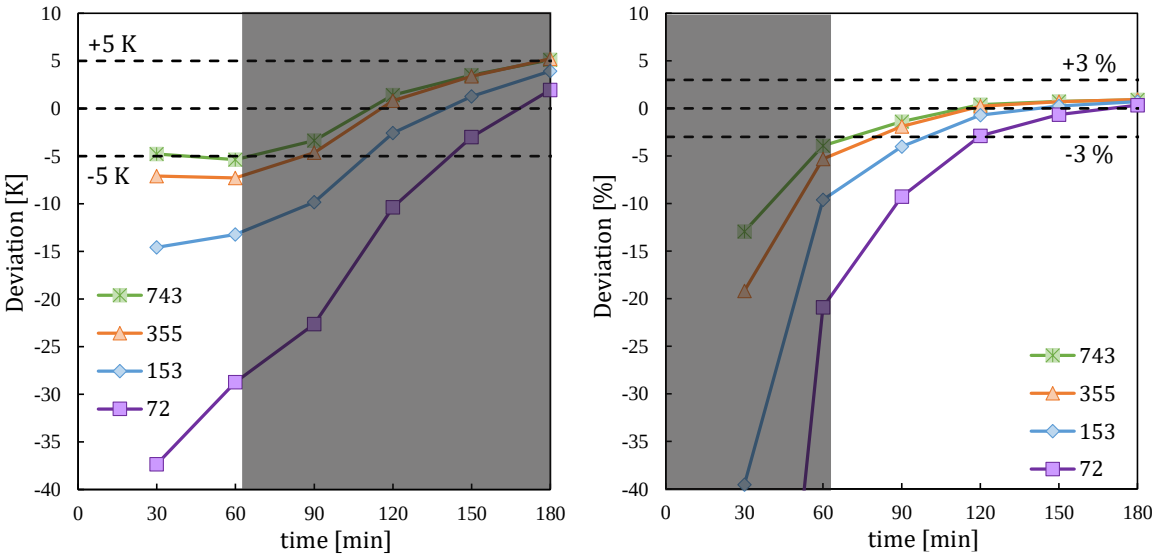

a) Degrees b) Percentage

Figure 39 – Differences between the results by SAFIR and the reference results, for quadrilateral meshes with different densities (expressed in number of nodes)

The analysis of the results in Figure 39 allows to conclude that having an unstructured mesh doesn't greatly affect the results obtained, as a mesh with 743 nodes presents very identical results to the ones obtained with a structured mesh with 625 nodes (see Figure 33), which fall inside the DIN limits for all the range of time instants studied.

2.2.6 Conclusions

Like in Example 1, the parametric analysis has shown that the solution satisfies the requirement of the standard, provided that the mesh used is sufficiently refined.

It was noticed that meshes with quadrilateral elements converged slightly but not significantly faster than triangular elements, while no significant differences appeared between unstructured and structured meshes.

2.3. Example 3

2.3.1 Keywords

Heat-transfer, conduction, convection, radiation, various material layers

2.3.2 Objective

The goal of this example is to analyse the heat transfer in a steel hollow section that is filled with a lightweight insulating material. The thermal conductive properties of steel are those of EN 1993-1-2 whereas the filling material has constant thermal properties.

2.3.3 Description of the problem

A square section with the characteristics defined in Figure 40 (not to scale) and Table 5 – Dimensions, material properties and boundary conditions for Example 3. is analysed. The temperature in the cross-section is uniform and equal to 0°C at time t = 0, when it is exposed to a gas with a temperature of 1000°C on all the edges. Heat transfer from the gas to the solid is by linear convection and by radiation. In order to validate the results, the temperature θ_0 calculated at the centre of the cross-section is compared to the reference values presented in the DIN EN1992-1-2 NA during 3 hours.

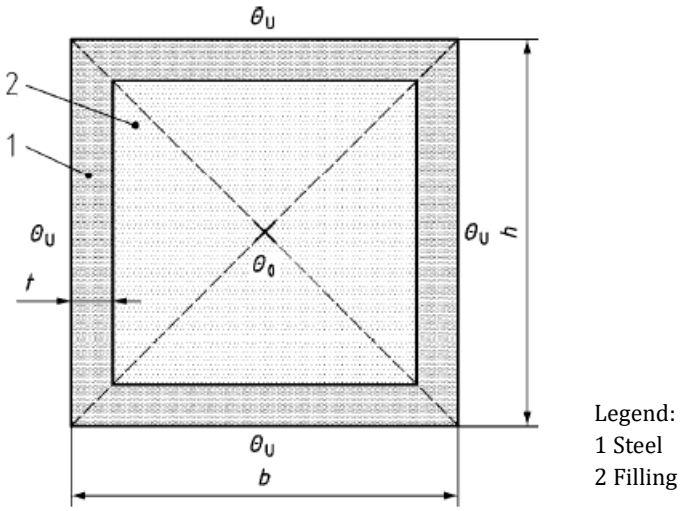

Figure 40 – Example 3: Heat-transfer in several layers

Table 5 – Dimensions, material properties and boundary conditions for Example 3.

Properties		Steel	Filling
Thermal conductivity λ	W / (m·K)	EN 1993-1-2	0.05
Specific heat cp	J / (kg·K)	EN 1993-1-2	1000
Density ρ	Kg / m³	EN 1993-1-2	50
Dimensions h, b, t	m	h = b = 0.201, t = 0.0005	
Coefficient of convection α_c	W / (m²·K)	10	
Emissivity $\varepsilon_{res} = \varepsilon_m . \varepsilon_f$	-	0.8	
Initial temperature in the cross-section Θ_{cs}	°C	0	0
Ambient temperature Θ_u	°C	1000	

2.3.4 Model and results (see folder DIN3_4)

A model with a structured mesh formed by 672 quadrilateral elements was created, which consists on a grid of 24 x 24 elements for the filling material, with the steel hollow section being defined with also 24 elements along each edge of the section and 1 element across the thickness. Each of these elements contains 2 Gauss points of integration, and the total number of nodes is 721.

The initial temperature in the structure was set to 0°C, and a frontier constraint of 1000°C was applied to all the faces of the cross-section according to *Figure 41*.

The PRECISION command was set to 1.0E-3. An INSULATION material with constant material properties according to Table 5 was used for the filling and a STEELEC3EN material for the hollow section (changing the heat transfer coefficients at the surface from the recommendation of EN 1993-1-2 to fit with the values of 10 Wm^2K and 0.8 of Table 3. The time step chosen was 10 s (final time / 1080).

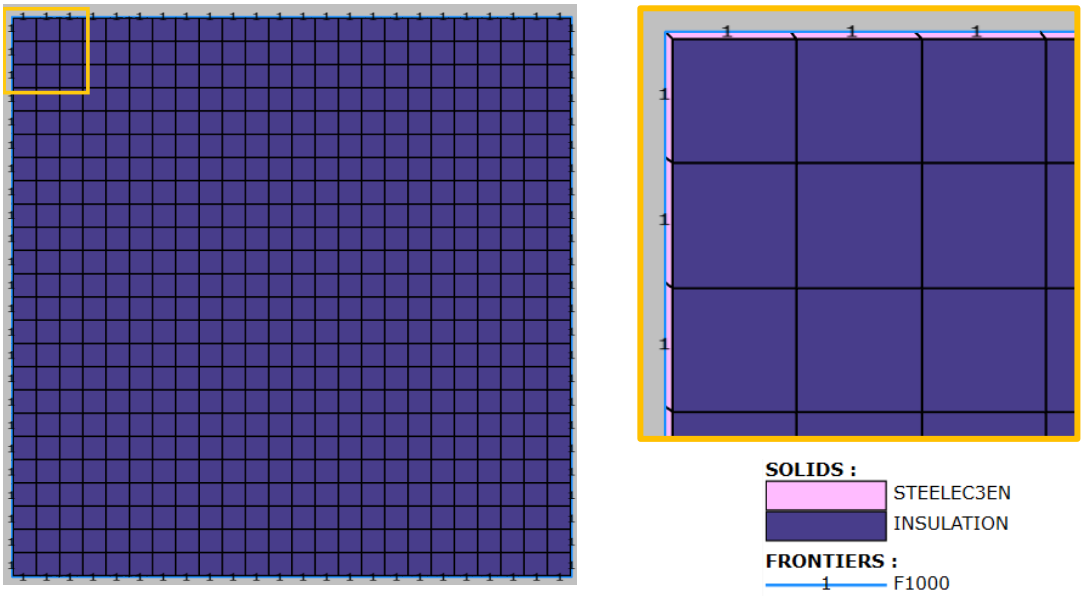

a) Overall view

b) Detail of the model at one corner

Figure 41 – Thermal model of the cross-section for (24 x 24 SOLID elements)

Figure 42 shows the temperature distribution for the final time of 180min. Table 6shows the deviations of the temperatures obtained by SAFIR when compared to those given as reference by the DIN.

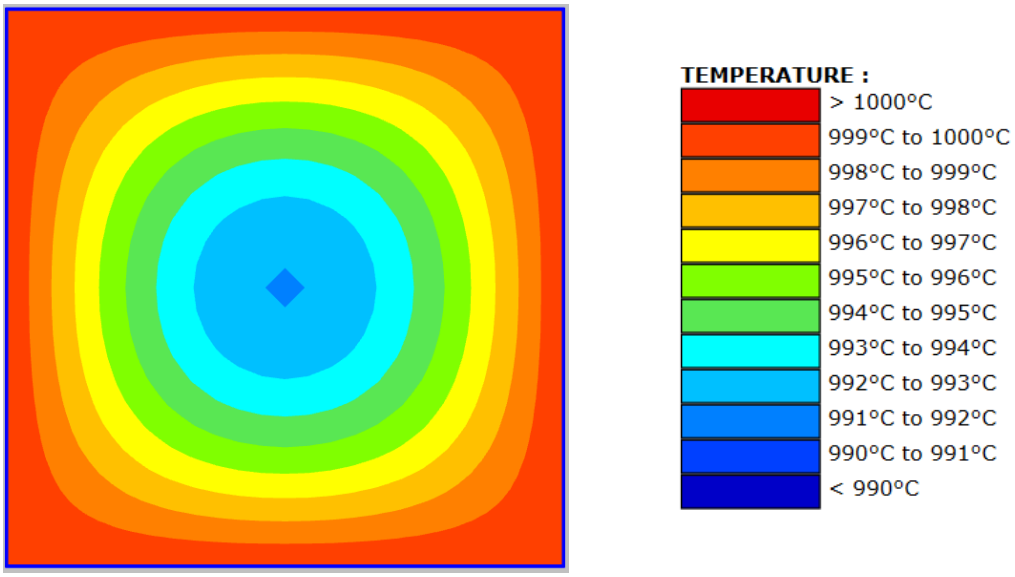

Figure 42 – Temperatures determined by SAFIR for Example 3, for t = 180min.

Table 6 – Temperature θ_0 for Example 3

Time	Reference temperature	Calculated temperature	Deviation	
t	Θ_0	Θ'_0	$(\Theta'_0 - \Theta_0)$	$(\Theta'_0 - \Theta_0) / \Theta_0 \cdot 100$
min	°C	°C	K	%
30	340.5	338.89	-1.61	-0.47
60	717.1	721.97	4.87	0.68
90	881.6	885.24	3.64	0.41
120	950.6	952.66	2.06	0.22
150	979.3	980.47	1.17	0.12
180	991.7	991.95	0.25	0.03
Limits			±5.00	±1.00

2.3.5 Conclusions

The deviations found were within the limits stipulated by the DIN, in absolute value as well as in relative value, for the whole duration of the simulation.

2.4. Example 4

2.4.1 Keywords

Thermal expansion, steel, homogenous temperature

2.4.2 Objective

The goal of this example is to analyse the thermal expansion of a steel element at different values of homogeneous temperature in a cross-section.

2.4.3 Description of the problem

A squared section with the characteristics defined in *Figure 43* and Table 7 is analysed. In order to validate the results, the thermal elongation Δl at the simply supported end of the member is determined and compared to the reference values presented in the DIN EN1992-1-2 NA.

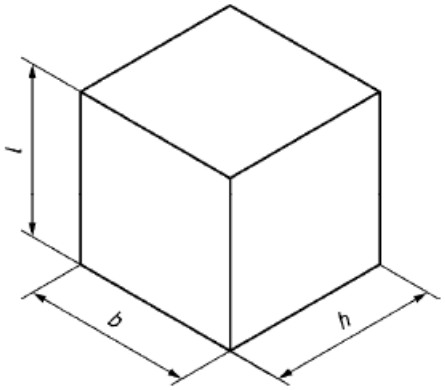

Figure 43 – Example 4: Statically assembled member

Table 7 – Dimensions, material properties and boundary conditions for Example 4

Properties		Steel
Dimensions l, h, b	mm	100
Stress-strain material law		EN 1993-1-2
Yield strength f_{yk}	N /mm²	355
Initial conditions	°C	20
Homogeneous temperature in the member Θ_u	°C	100, 300, 500, 600, 700, 900
Thermal expansion	-	EN 1993-1-2

2.4.4 Model and results (see folder DIN4_4)

In this example the calculations were performed using BEAM, TRUSS, SHELL and SOLID elements, in order to get those different formulations validated.

No thermal analysis is presented here. The prescribed temperatures have been directly introduced in the relevant files for the structural analysis to be performed.

BEAM elements

A 2D mechanical model with 1 BEAM element that is free to expand was created and exposed, unloaded, to the prescribed temperature fields.

In *Figure 44* a representation of the thermal elongation determined by SAFIR is shown (in the Figure the elongation is causing the right support to move horizontally).

Figure 44 – Thermal elongation determined by SAFIR for Example 4, for t = 900°C, using a BEAM element

Table 8 shows the deviations of the temperatures obtained by SAFIR when compared to those given as reference by the DIN.

Table 8 – Thermal elongation Δl for *Example 4*, using a BEAM element

Temperature	Reference extension	Calculated extension	Deviation	
Θ	Δl	Δl'	(Δl' - Δl)	(Δl' - Δl) / Δl · 100
°C	mm	mm	mm	%
100	0.09984	0.0998	-0.00004	-0.04
300	0.37184	0.372	0.00016	0.04
Limit (Θ ≤ 300°C)			±0.05	
500	0.67584	0.676	0.00016	0.02
600	0.83984	0.84	0.00016	0.02
700	1.01184	1.01	-0.00184	-0.18
900	1.18000	1.18	0.00000	0.00
Limit (Θ > 300°C)				±1.00

TRUSS elements

A 2D mechanical model with 1 TRUSS element that is free to expand was created and exposed, unloaded, to the prescribed temperature fields.

In *Figure 45 – Thermal elongation determined by SAFIR for Example 4, for t = 900°C, using a TRUSS element* a representation of the thermal elongation determined by SAFIR is shown (in the Figure the elongation is causing the right support to move horizontally).

Figure 45 – Thermal elongation determined by SAFIR for Example 4, for t = 900°C, using a TRUSS element

Table 9 shows the deviations of the temperatures obtained by SAFIR when compared to those given as reference by the DIN.

Table 9 – Thermal elongation Δl for *Example 4,* using a BEAM element

Temperature	Reference extension	Calculated extension	Deviation	
Θ	Δl	Δl'	(Δl' - Δl)	(Δl' - Δl) / Δl · 100
°C	mm	mm	mm	%
100	0.09984	0.0998	-0.00004	-0.04
300	0.37184	0.371	-0.00084	-0.23
Limit (Θ ≤ 300°C)			±0.05	
500	0.67584	0.674	-0.000184	-0.27
600	0.83984	0.836	-0.000384	-0.46
700	1.01184	1.01	-0.00184	-0.18
900	1.18000	1.17	-0.01000	-0.85
Limit (Θ > 300°C)				±1.00

SHELL elements

A 3D mechanical model with 9 SHELL elements (3x3) that is free to expand was created and exposed, unloaded, to the prescribed temperature fields.

The visualization in DIAMOND of the displacements obtained by SAFIR in one of the directions is shown in Figure 46 (the same results were obtained for the expansion in both directions).

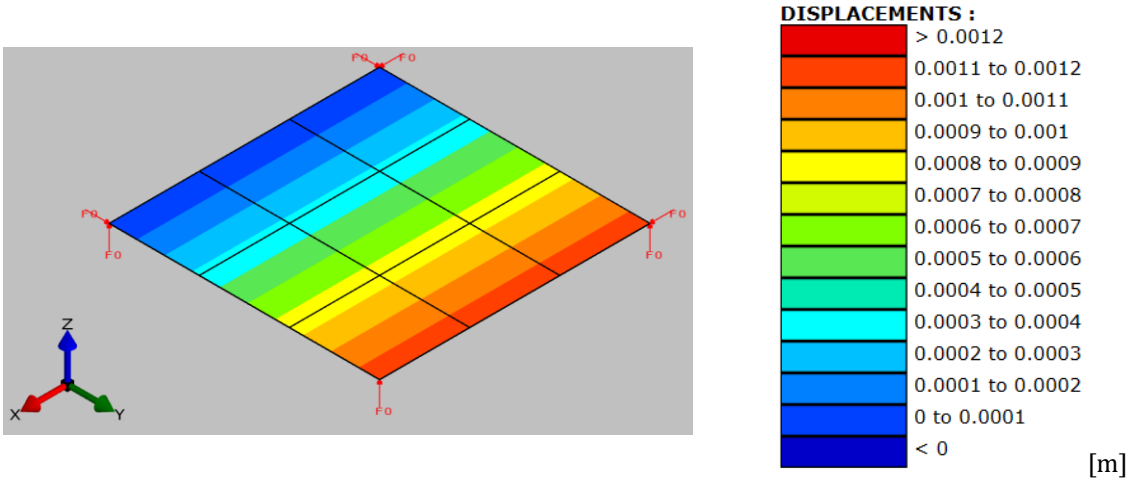

Figure 46 – Thermal elongation in Y-direction determined by SAFIR for Example 4, for t = 900°C, using SHELL elements

Table 10 shows the deviations of the temperatures obtained by SAFIR when compared to those given as reference by the DIN.

Table 10 – Thermal elongation Δl for Example 4, using SHELL elements

Temperature	Reference extension	Calculated extension	Deviation	
Θ	Δl	Δl'	(Δl' - Δl)	(Δl' - Δl) / Δl · 100
°C	mm	mm	Mm	%
100	0.09984	0.0998	-0.00004	-0.04
300	0.37184	0.371	-0.00084	-0.23
Limit (Θ ≤ 300°C)			±0.05	
500	0.67584	0.674	-0.000184	-0.27
600	0.83984	0.836	-0.000384	-0.46
700	1.01184	1.01	-0.00184	-0.18
900	1.18000	1.17	-0.01000	-0.85
Limit (Θ > 300°C)				±1.00

SOLID elements

A 3D mechanical model with 1 SOLID element that is free to expand was created and exposed, unloaded, to the prescribed temperature fields.

The visualization in DIAMOND of the displacements obtained by SAFIR in one of the directions is shown in Figure 47 (the same results were obtained for the expansion in all 3 directions).

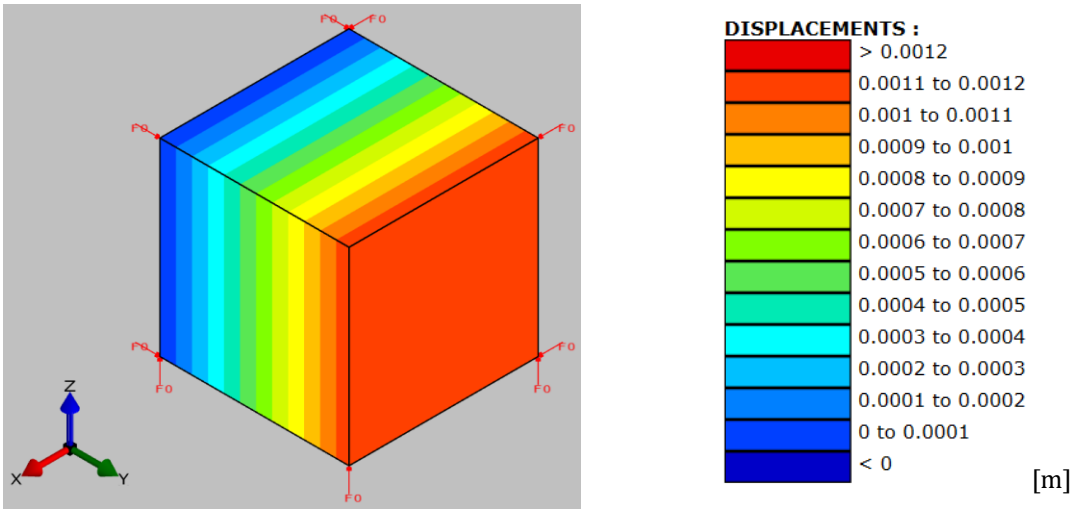

Figure 47 – Thermal elongation in Y-direction determined by SAFIR for Example 4, for t = 900°C, using a SOLID element

Table 11 shows the deviations of the temperatures obtained by SAFIR when compared to those given as reference by the DIN.

Table 11 – Thermal elongation Δl for Example 4, using a SOLID element

Temperature	Reference expansion	Calculated expansion	Deviation	
Θ	Δl	Δl'	(Δl' - Δl)	(Δl' - Δl) / Δl · 100
°C	mm	mm	mm	%
100	0.00984	0.0998	-0.00004	-0.04
300	0.37184	0.372	0.00016	0.04
Limit (Θ ≤ 300°C)			±0.05	
500	0.67584	0.676	0.00016	0.02
600	0.83984	0.84	0.00016	0.02
700	1.01184	1.01	-0.00184	-0.18
900	1.18000	1.18	0.00000	0.00
Limit (Θ > 300°C)				±1.00

2.4.5 Conclusions

The results calculated for both types of elements are within the limits stipulated by the DIN. It may appear as inconsistent that, in one single software, the thermal expansion is not exactly the same for all types of elements. Indeed, for 900°C, for example, the BEAM and the SOLID finite elements yield an expansion of 1.18 mm, which is exactly the expected value, whereas the TRUSS and the SHELL finite elements yield a value of 1.17 mm.

The reason lies in the fact that the axial strain is calculated based on a linearized expression in the SOLID elements (because they are written in a small displacements formulation) and in the BEAM finite elements (because these are expected to deflect essentially in bending rather than in elongation).

$$\varepsilon = \frac{l - l_i}{l_i}$$

On the contrary, for the TRUSS elements where elongation is the sole deformation and in SHELL elements that can also work as membrane elements, the more correct nonlinear expression is being used.

$$\varepsilon = \frac{l^2 - {l_i}^2}{2\,{l_i}^2}$$

It can be verified that, with an elongation of 1.17 mm from an initial length of 100 mm, the second expression yields a strain equal to 1.1768 %. If, by multiplying the length of the specimen by a factor of 10, one gains access to an additional significant digit, the elongation for the BEAM and the SOLID elements is found as 1.173 mm, which yields a strain of 1.1799 %.

The results are thus consistent with the fact that thermal strain of steel in SAFIR is calculated in the same manner for all element types, in full accordance with the recommendation of EN 1993-1-2.